IEEE Access
Multidisciplinary | Rapid Review | Open Access Journal

Received September 20, 2019, accepted October 10, 2019, date of publication October 17, 2019, date of current version October 31, 2019.

Digital Object Identifier 10.1109/ACCESS.2019.2948034

A New Array Pseudolites Technology for High Precision Indoor Positioning

XINGLI GAN[1,2], BAOGUO YU[1,2], XIANPENG WANG[3], YONGQIN YANG[3], RUICAI JIA[1,2], HENG ZHANG[1,2], CHUANZHEN SHENG[1,2], LU HUANG[1,2], AND BOYUAN WANG[1,2]

[1]The 54th Research Institute of China Electronics Technology Group Corporation, Shijiazhuang 050081, China
[2]State Key Laboratory of Satellite Navigation System and Equipment Technology, Shijiazhuang 050081, China
[3]State Key Laboratory of Marine Resource Utilization in South China Sea, Hainan University, Haikou 570228, China

Corresponding author: Yongqin Yang (yangyq@hainu.edu.cn)

This work was supported in part by the Natural Science Foundation of Hainan Province under Grant 617059, and in part by the project Indoor Hybrid Intelligent Positioning and Indoor GIS Technology, which is part of State's Key Project and Development Plan of China, under Contract 2016YFB0502100 and Contract 2016YFB0502101.

ABSTRACT Global Satellite Navigation System (GNSS) can't provide normal location service in the indoor environment because the signal can be blocked by buildings. The pseudolites system can supplement GNSS, especially in the indoor environments. A new indoor array pseudolites system is introduced, its multi-channel transmitter has an identical clock source. The high-precision Doppler positioning method based on Z-fixed Known Point Initialization (Z-KPI) is developed without ambiguity resolution. Some static and dynamic tests are conducted to evaluate the positioning accuracy of this new method. In the static testing, the average Doppler measurement error is 1×10-5 m/s, which lays the foundation of the high precision velocity measurement, and the average positioning error is 0.02 m in X axis, 0.004 m in Y axis, and the average velocity error is 3.28×10^{-5} m/s in X axis, 1.94×10^{-5} m/s in Y axis. In the dynamic test, the maximum positioning error is 0.39 m in X axis, 0.34 m in Y axis. Finally, the reason for adopting the Z-fixed KPI algorithm is explained by the horizontal dilution of precision (HDOP), meanwhile, the influence of the known initialization point error on indoor positioning accuracy is analyzed, when a deviation from −1.5 m to 0.9 m is added to the Z-axis of the KPI, the maximum positioning error is 0.311 m in X axis, 0.08 m in Y axis; when the horizontal deviation tolerance of the KPI is set from - 0.5 m to 0.5 m, the maximum horizontal positioning error is less than 0.5 m.

INDEX TERMS Indoor array pseudolites, positioning, velocity, Doppler observation, Z-fixed KPI.

I. INTRODUCTION

With the development of LBS in urban area, the indoor positioning system has been getting a lot of attention in the academic and commercial fields. Global Satellite Navigation System provides a high-precision, wide-area coverage and high-continuity positioning service for personal smartphones in the outdoor environment. However, GNSS can't provide the normal location service in the indoor environment because the signal can be blocked by buildings. In recent years, multiple pseudolites systems, such as IMES and Locata, have been supplemented to GNSS, especially for the indoor environments. GNSS-like signals can be used by the pseudolites system [1]–[6], and the signals can be tracked by a commercial GNSS receiver with minor modifications for the positioning software.

Several pseudolites systems have been proposed to achieve high-precision indoor positioning. The indoor messaging system (IMES) developed by Japanese Aerospace Exploration Agency [7]–[9] is based on the proximity location, and the positioning error of IMES is usually from 5 meters to 10 meters. The multi-channel pseudolites with array antenna is proposed by Fujii *et al.* [10], the array antenna consists of three antennas which are located at the interval of the half-wavelength of the GPS L1 carrier wave, i.e., at 95.15 mm from each other. It does not require the time synchronization and indoor multipath problems of indoor positioning with conventional pseudolites, and the positioning accuracy varies from centimeter- to meter-level according to the geometric relation between the antenna array and the receiver. However, the multi-channel pseudolites is difficult to

The associate editor coordinating the review of this manuscript and approving it for publication was Guan Gui.

support dynamic positioning and has only a $4m \times 4m$ positioning coverage area. Another multi-channel pseudolite called the GNSS repeater has been proposed by Niwa [11]–[14], which realizes indoor positioning using carrier phase difference method with the base and rover stations. A combined approach of Doppler and carrier-based hyperbolic positioning with a multi-channel GPS-pseudolite for indoor localization has also been proposed by Fujii *et al.* [23], an state equation of three dimensional(3-D) receiver's position and orientation, and ambiguity is established, an observation equation for Doppler positioning is used to estimate the offset of three dimensional(3-D) position and orientation, a nonlinear observation equation for carrier phase difference between pseudolites is used to estimate ambiguity, therefore, it needs to overcome such problems as ambiguity resolution, non-linear observation equation, positioning stability and real-time, etc.. The most famous indoor pseudolites system is produced by Locata Corporation [2], [15], [16], which consists of a network (LocataNet) of time-synchronised transceivers (LocataLites), and it has the potential to allow point positioning with sub-cm precision (using carrier phase) for a mobile unit. To achieve synchronization among all the pseudolites' clock, TimeLoc technology can provide an autonomously synchronized network, which requires the additional ranging signals (code and carrier) and the visibility between pseudolites. Therefore, it is very difficult to apply and cover wide areas in the indoor environment.

Due to severe multipath effects, the high-precision indoor pseudolites positioning (cm-level) is difficult to use pseudo-range observations. Several methods of using carrier phase observation have been developed and the core problem is how to fix the ambiguities. The ambiguity function method [17] and LAMBDA [18], [19] can be usually used to solve the fixed ambiguities for GNSS outdoor positioning, but the pseudolites can't use those methods because of the poor accuracy of the pseudo-range and the bad geometry structure in the indoor environment. Therefore, the KPI method [20], [21] has been generally adopted to solve ambiguities. In many cases, even if the known points reach centimeter-level precision, it still cannot pass the ambiguity validation [22]. Because the complexity of the LAMBDA method of pseudolites system will consume computing resources of processor and power of smartphones, it is not suitable for the indoor pedestrian navigation using smartphones.

In the following sections, a new indoor array pseudolites system is introduced, which overcomes the problem of complex time synchronization of the traditional pseudolites [24], each signal of the array pseudolites is generated at the same time by the pulse per second (1PPS), then the clock drift of pseudolites should be same. In addition, we developed the Z-fixed KPI algorithm based on the high-precision carrier phase and Doppler measurements to calculate the velocity of receiver, then, the receiver position of current epoch is computed by the position of previous epoch, the speed of current epoch and the time interval of the observation. The new method has two advantages: first, it does not need to solve the integer ambiguity, has less computation and is suitable for smartphones; second, the centimeter-level positioning can be achieved by using the high precision Doppler and carrier phase observation. Finally, the reason for adopting the Z-fixed algorithm is explained, and the indoor positioning accuracy is analyzed.

II. POSITIONING THEORY

A. INDOOR ARRAY PSEUDOLITES SYSTEM

Fig.1 illustrates the system structure of indoor array pseudolites consisting of three parts: the multi-channel signal transmitter, array antennas and user terminal.

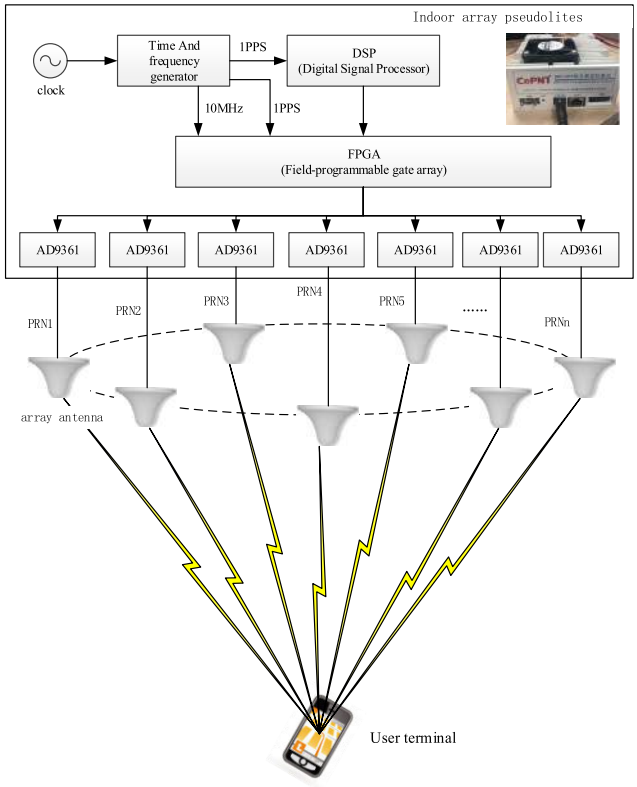

FIGURE 1. Illustration of proposed system.

1) INDOOR ARRAY PSEUDOLITES TRANSMITTER

Each channel of the indoor array pseudolites system transmits a signal with a unique C/A code modulated on GPS L1 and BDS B1 carrier waves. The signal properties of the pseudolites are shown in TABLE 1. The signals of array pseudolites are generated at the same time by 1PPS, and the clock drift of each channel for indoor array pseudolites can be same. In this way, the complex time synchronization can be avoided.

2) USER TERMINAL

Fig.2 shows the user terminal including an antenna, a Bluetooth module, and a commercialized receiver chip (such as ublox M8T/P, Unicorecomm UC6226). The GNSS chip tracks signals of indoor array pseudolites and provides raw

TABLE 1. Signal properties of indoor array pseudolites.

Item	L1	B1
Center Frequency	1575.42MHz	1561.098MHz
Bandwidth	2.046MHz	4.092MHz
PRN ID	172-183	172-183
Modulation	TDMA+BPSK	TDMA+BPSK
Polarization	RHCP	RHCP

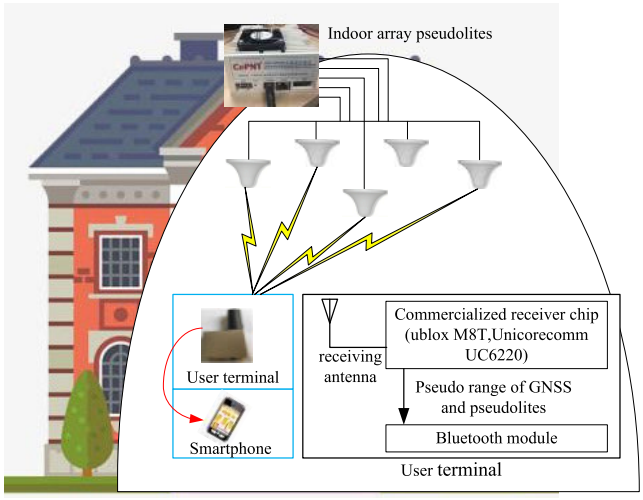

FIGURE 2. Architecture of user terminal.

observations of carrier-phase and Doppler. The raw observations from the GNSS chip are transmitted to smartphone via Bluetooth signal. Then, position and speed of receiver are computed on smartphone processors.

B. ALGORITHM

1) VELOCITY OF DOPPLER OBSERVATION

The Doppler Observation equation between receiver u and transmitting channel i of indoor array pseudolites can be written as:

$$\frac{c}{f}\cdot D_u^i = \dot{R}_u^i + c\cdot d\dot{t}_u - c\cdot d\dot{t}^s + \dot{\varepsilon}_u^i \tag{1}$$

where D_u^i is the Doppler measurement between receiver u and transmitting channel i of indoor array pseudolites; c is the speed of light; f is the frequency of navigation signal; $\dot{R}_u^i$ is the change rate of geometric distance between receiver u and transmitting antenna i of pseudolites; $d\dot{t}_u$ is the rate of receiver clock biases; $d\dot{t}^s$ is the rate of pseudolites clock biases; $\dot{\varepsilon}_u^i$ is the combined error residual.

The rate of geometric distance $\dot{R}_u^i$ can be written as:

$$\dot{R}_u^i = \frac{(x_u - x^i)(\dot{x}_u - \dot{x}^i) + (y_u - y^i)(\dot{y}_u - \dot{y}^i) + (z_u - z^i)(\dot{z}_u - \dot{z}^i)}{\sqrt{(x_u - x^i)^2 + (y_u - y^i)^2 + (z_u - z^i)^2}} \tag{2}$$

where x_u, y_u, z_u are the three-dimensional coordinates of receiver u; $\dot{x}_u$, $\dot{y}_u\dot{z}_u$ are the velocity of receiver u, which can be solved with four Doppler measurements and least squares estimation; x^i, y^iz^i are the three-dimensional position of pseudolites' transmitting antenna i; $\dot{x}^i = 0$, $\dot{y}^i = 0$, $\dot{z}^i = 0$ are the velocity of indoor stationary pseudolites.

Inserting (2) into (1) gives:

$$\frac{c}{f}\cdot D_u^i = \frac{(x_u - x^i)\cdot\dot{x}_u + (y_u - y^i)\cdot\dot{y}_u + (z_u - z^i)\cdot\dot{z}_u}{\sqrt{(x_u - x^i)^2 + (y_u - y^i)^2 + (z_u - z^i)^2}} + c\cdot d\dot{t}_u - c\cdot d\dot{t}^s + \dot{\varepsilon}_u^i \tag{3}$$

The observation equations of indoor array pseudolites can be expressed as the following matrix form:

$$\begin{bmatrix} \frac{x_u - x^1}{R_u^1} & \frac{y_u - y^1}{R_u^1} & \frac{z_u - z^1}{R_u^1} & 1 \\ \frac{x_u - x^2}{R_u^2} & \frac{y_u - y^2}{R_u^2} & \frac{z_u - z^2}{R_u^2} & 1 \\ \cdots & \cdots & \cdots & \cdots \\ \frac{x_u - x^n}{R_u^n} & \frac{y_u - y^n}{R_u^n} & \frac{z_u - z^n}{R_u^n} & 1 \end{bmatrix} \cdot \begin{bmatrix} \dot{x}_u \\ \dot{y}_u \\ \dot{z}_u \\ c\cdot d\dot{t}_u - c\cdot d\dot{t}^i \end{bmatrix} = \begin{bmatrix} \frac{c}{f}\cdot D_u^1 \\ \frac{c}{f}\cdot D_u^2 \\ \cdots \\ \frac{c}{f}\cdot D_u^n \end{bmatrix} + \begin{bmatrix} \dot{\varepsilon}_u^1 \\ \dot{\varepsilon}_u^2 \\ \cdots \\ \dot{\varepsilon}_u^n \end{bmatrix} \tag{4}$$

The matrix on the left-hand side of (4) can be defined as **G,** and the two column vectors on the right-hand side are defined as **b** and $\boldsymbol{\varepsilon}$ respectively, then (4) is written as:

$$\mathbf{G}\cdot\mathbf{v}_{u,s} = \mathbf{b} + \boldsymbol{\varepsilon} \tag{5}$$

If the initial value of $\mathbf{v}_u$ is used for the solution-updating process, the Newton-Raphson method is described as $\mathbf{v}_{u,0} = (\dot{x}_{u,0}, \dot{y}_{u,0}, \dot{z}_{u,0})$. The least squares updated solution can be represented as:

$$\Delta\mathbf{v}_{u,0} = (\mathbf{G}^T\mathbf{G})^{-1}\mathbf{G}^T\mathbf{b} \tag{6}$$

Then the estimated velocity can be updated iteratively according to

$$\hat{\mathbf{v}}_{u,1} = \mathbf{v}_{u,0} + \Delta\mathbf{v}_{u,0} \tag{7}$$

2) POSITION BASED ON VELOCITY ESTIMATION

The estimated position $\mathbf{r}_{u,1}$ can be written as:

$$\mathbf{r}_{u,1} = \mathbf{r}_{u,0} + \hat{\mathbf{v}}_{u,1}\cdot\Delta t \tag{8}$$

where $\mathbf{r}_{u,0}$ is the initial value of $\mathbf{r}_u$ which is the coordinate of receiver u. Δt represents time interval of the observation.

3) Z-FIXED KNOWN POINT INITIALIZATION METHOD

A new method is proposed in the paper and the procedure of the z-fixed Known Point Initialization (KPI) algorithm is shown in Fig.3.

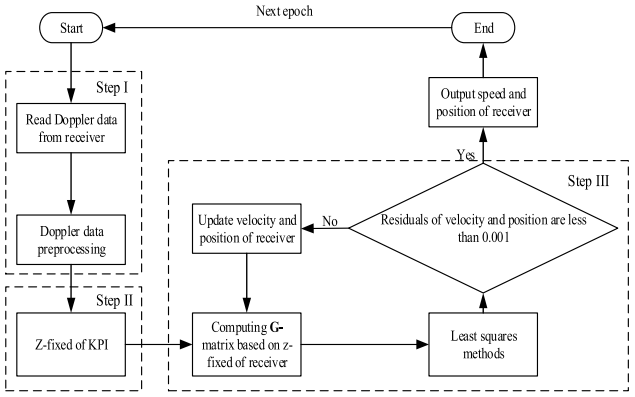

FIGURE 3. The procedure of the Z-fixed KPI algorithm.

Step I:

The first step of our approach is to compute the carrier-phase rate in (9), detect and eliminate abnormal Doppler measurements.

$$\dot{\phi}_k^i = \frac{\phi_{k+\Delta t}^i - \phi_k^i}{\Delta t} \tag{9}$$

where ϕ is the carrier-phase observation; superscript i represents the transmitting channel of pseudolites; k represents observation epoch and Δt represents time interval of the observation.

Step II:

The starting point of receiver is initialized and its three-dimensional (3D) coordinates are known. The coordinates of Z-axis are set to a constant during the measurements of position and velocity. Therefore, our approach is called the Z-fixed KPI algorithm.

Step III:

The Newton-Raphson method in (6) and (8) is used to estimate velocity and position of user receiver.

III. POSITIONING EXPERIMENT

A. EXPERIMENTAL SETUP

The performance of the proposed indoor positioning system is evaluated in a room as shown in Fig.4, the size of the room is about 39 meters long and 25 meters wide. The antenna coordinates of pseudolites and receiver were surveyed precisely with a total station, the precise position of receiver is known as a ground truth, which is compared with the positioning result of pseudolites and ultra-wideband (UWB).

Fig.5 shows the array antenna of 3 meters diameter, based on a circular array of eight Right-Hand Circularly Polarized (RHCP) antenna elements, and the height of the antenna element is 8 meters above the ground.

B. EXPERIMENTAL RESULTS

The static test is performed firstly. If the speed of the receiver is zero, (3) can be written as:

$$\frac{c}{f} \cdot D_u^i = c \cdot d\dot{t}_u - c \cdot d\dot{t}^s + \dot{\varepsilon}_u^i \tag{10}$$

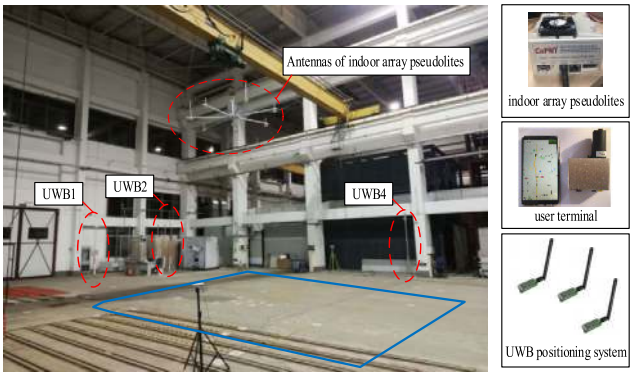

FIGURE 4. Experimental environment of indoor array pseudolites.

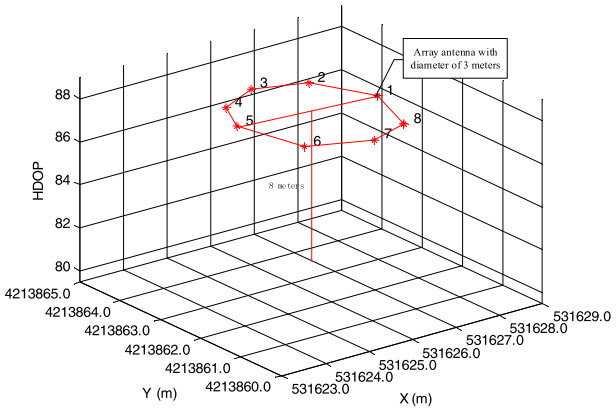

FIGURE 5. The antennas' distribution of indoor array pseudolites.

Assumming that the combined error residual $\dot{\varepsilon}_u^i$ is Gauss white noise, the rate of pseudolites and receiver clock biases can be calculated as:

$$c \cdot d\dot{t}_u^s = c \cdot d\dot{t}_u - c \cdot d\dot{t}^s = \frac{\sum_{i=1}^{n} \frac{c}{f} \cdot D_u^i}{n} \quad \text{and}$$

$$\dot{\varepsilon}_u^i = D_u^i - \frac{\sum_{i=1}^{n} \frac{c}{f} \cdot D_u^i}{n} \tag{11}$$

where n is the number of signal channels received by the receiver at the same epoch.

Fig.6 shows the Doppler error by the static test of the indoor array pseudolites. The average Doppler measurement error $\dot{\varepsilon}_u^i$ is 1×10^{-5} m/s, the standard deviation (Std) of Doppler measurement error is from 0.002 m/s to 0.004 m/s. It is can be concluded that a high-precision velocity and positioning can be achieved by the millimeter-scale Doppler measurement.

Fig.7 shows the results of 2-D static positioning and velocity for pseudolites, the average positioning error is 0.02 m in X axis, 0.004 m in Y axis. It is shown that the average velocity error is 3.28×10^{-5} m/s in X axis, 1.94×10^{-5} m/s in Y axis. The standard deviation of the X-axis and Y-axis positioning errors are 0.0037 m and 0.0044 m, respectively.

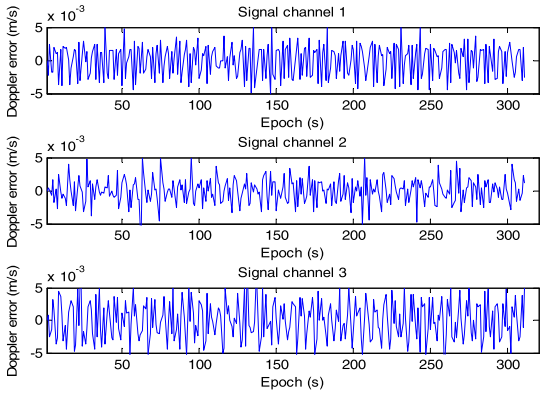

FIGURE 6. Doppler error by static test of indoor array pseudolites.

The standard deviation of the X-axis and Y-axis velocity errors are 0.011 m/s and 0.0077 m/s, respectively.

To test the accuracy of dynamic positioning, two methods are used: One is the statistical method based on known points, by calculating the deviation of the true and measured position of endpoints; the other is the positioning trajectory comparison method between UWB and pseudolites.

Fig.8 shows the dynamic positioning results for eight test paths (straight path from 68 to 69 and from 18 to 43, triangular path from 68, 69, 66 to 68, random path from 47 to 47, from 47 to 38, and from 99 to 99). The initialized known points reach centimeter-level precision by Total Station, and the coordinates of Z-axis produces random deviation less than 0.2 meters during people's movement. The test receiver can reach the end point from the starting point in each path, its positioning trajectory is continuous and stable without any big jump. It can be concluded that the coordinate of Z axis can be assigned an approximate value for pedestrian indoor positioning to reduce the complexity of pedestrian operation and navigation.

TABLE 2 shows the dynamic positioning error, the maximum positioning error is 0.39 m in X axis, and 0.34 m in Y axis. The maximum horizontal positioning error is 0.52 m, and the average horizontal positioning error is 0.21 m.

Fig.9 shows the comparison of position trajectories between UWB and pseudolites. The results show that the proposed indoor positioning system has a similar accuracy with the UWB.

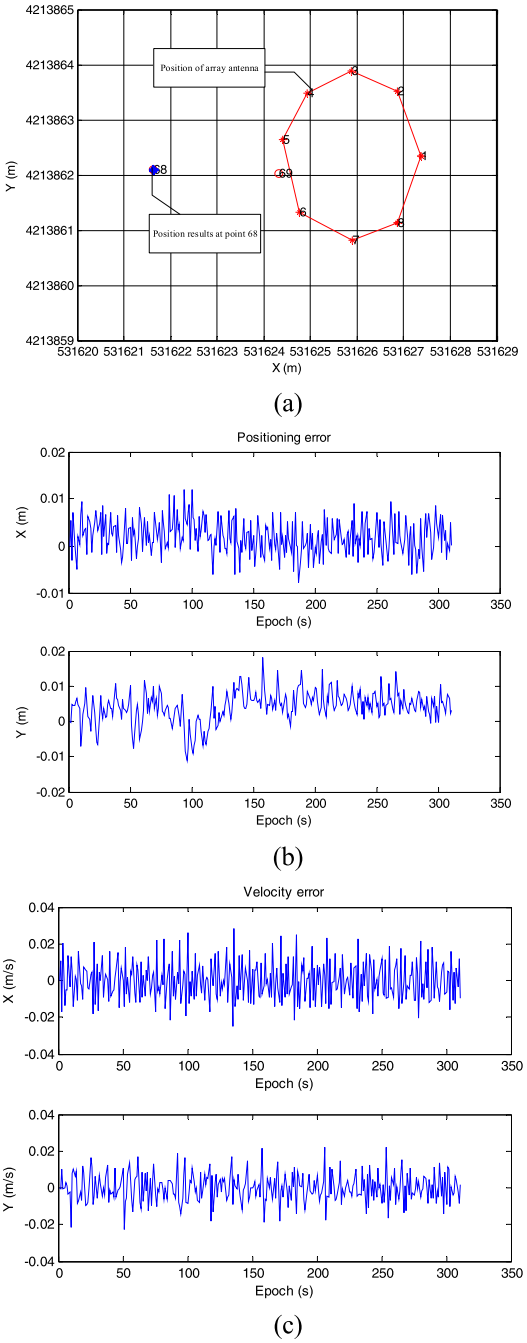

FIGURE 7. Static test of indoor array pseudolites: (a) positioning results, (b) positioning error and (c) velocity error.

IV. POSITIONING ERROR OF INDOOR ARRAY PSEUDOLITES

The reason for adopting the Z-fixed algorithm is explained by the HDOP in this section. Besides, the influence of the known initialization point error on indoor positioning accuracy is analyzed.

A. DILUTION OF PRECISION

1) 3D AND 2D HDOP

The three dimensional (3D) velocity error is estimated by the ''dilution of precision'' (DOP) [25], which can be expressed as:

$$\mathrm{cov}(\Delta r_u) = \sigma_\varepsilon^2 \cdot (\mathbf{G}^T\mathbf{G})^{-1} \tag{12}$$

If $(\mathbf{G}^T\mathbf{G})^{-1}$ is defined as $\mathbf{H}$, the DOP can be expressed as the diagonal elements of $\mathbf{H}$ as follows

$$\mathbf{H} = \begin{bmatrix} xDOP^2 & & & \\ & yDOP^2 & & \\ & & zDOP^2 & \\ & & & tDOP^2 \end{bmatrix} \tag{13}$$

TABLE 2. Dynamic positioning error.

Path	True position of endpoints		Measured position of endpoints		Error of X (m)	Error of Y (m)
	X (m)	Y (m)	X (m)	Y (m)		
68-69	531624.30	4213862.03	531624.31	4213862.03	0.01	0.00
18-43	531628.66	4213859.69	531628.44	4213860.00	0.22	0.31
47-47	531622.64	4213860.09	531622.87	4213860.16	0.23	0.07
47-38	531623.31	4213868.57	531623.30	4213868.22	0.01	**0.34**
38-47	531622.64	4213860.09	531622.69	4213860.22	0.05	0.13
68-69-66-68	531621.63	4213862.09	531621.23	4213862.15	**0.39**	0.06
99-99	531623.43	4213866.78	531623.41	4213866.99	0.02	0.22

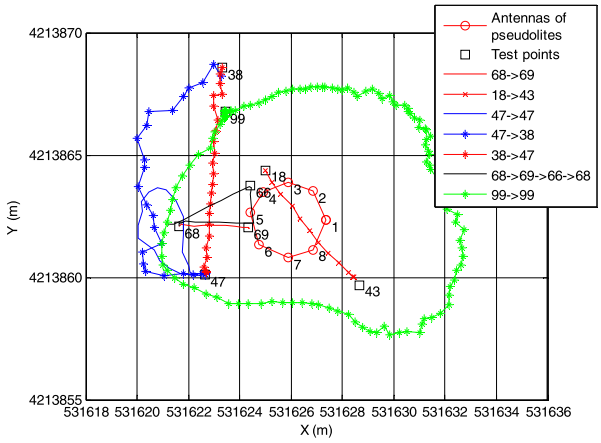

FIGURE 8. Dynamic positioning results of indoor array pseudolites.

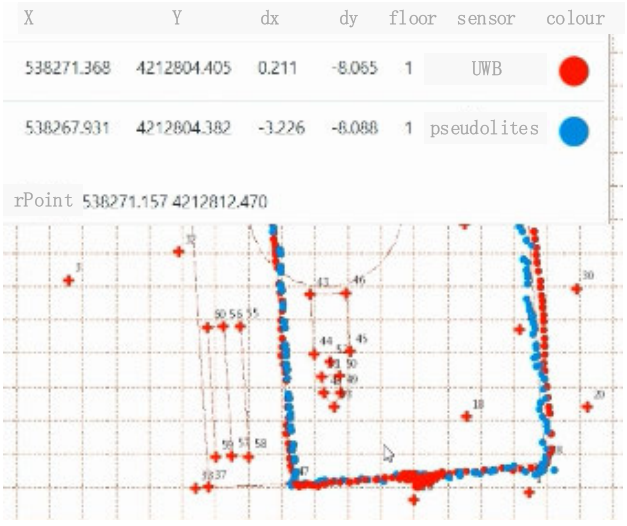

FIGURE 9. Comparison of position trajectories between UWB and pseudolites.

The variance of 3D-velocity error is given by

$$\begin{aligned}\sigma_{v_x}^2 &= \sigma_\varepsilon^2 \cdot xDOP^2 \\ \sigma_{v_y}^2 &= \sigma_\varepsilon^2 \cdot yDOP^2 \\ \sigma_{v_z}^2 &= \sigma_\varepsilon^2 \cdot zDOP^2 \\ \sigma_{v_t}^2 &= \sigma_\varepsilon^2 \cdot tDOP^2 \end{aligned} \tag{14}$$

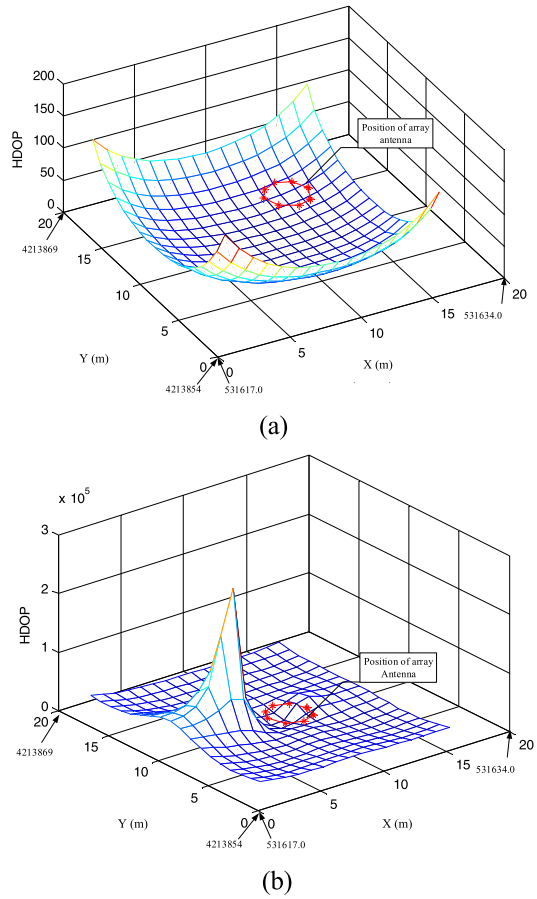

FIGURE 10. Indoor array pseudolites: (a) 2D-velocity HDOP and (b) 3D-velocity HDOP.

HDOP is defined as:

$$\sigma_{v_{xy}} = \sqrt{\sigma_{v_x}^2 + \sigma_{v_y}^2} = \sigma_\varepsilon \cdot \sqrt{xDOP^2 + yDOP^2} = \sigma_\varepsilon \cdot HDOP \tag{15}$$

For the indoor array pseudolites, the z-fixed KPI algorithm can be used to solve the two dimensional (2D) velocity of receiver, then the diagonal elements of $\mathbf{H}$ can be written as:

$$\mathbf{H} = \begin{bmatrix} xDOP^2 & & \\ & yDOP^2 & \\ & & tDOP^2 \end{bmatrix} \tag{16}$$

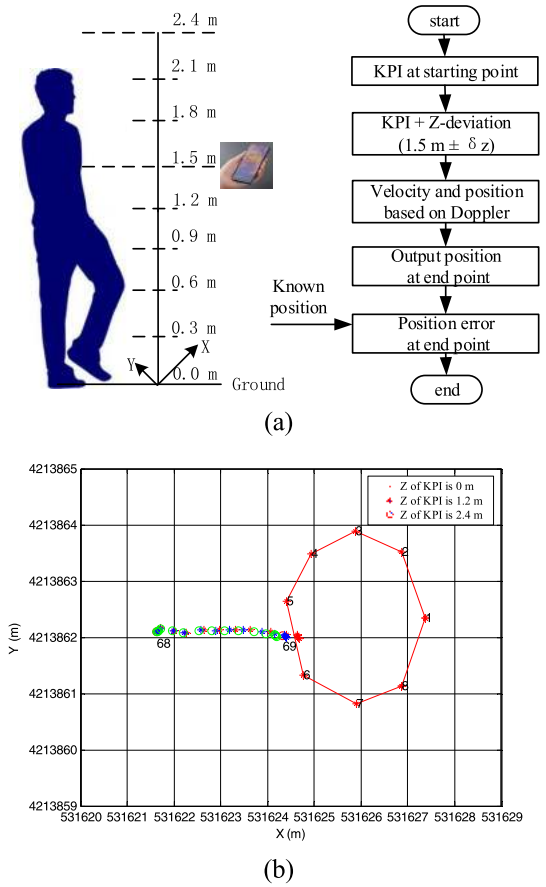

FIGURE 11. Z-axis deviation of known point: (a) analytic procedure and (b) positioning result.

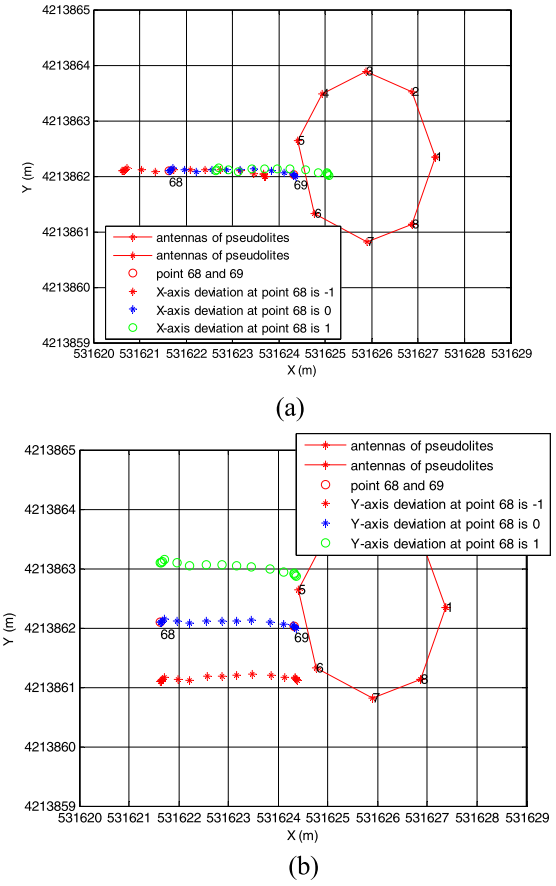

FIGURE 12. Positioning error: (a) X-axis deviation of known point and (b) Y-axis deviation of known point.

2) HDOP ANALYSIS

According to the installation parameters of array antenna as shown in Fig.5, the 2D-velocity HDOP of indoor array pseudolites is given in Fig.10 (a), which ranges from 10 to 110. The 3D-velocity HDOP is given in Fig.10 (b), which drastic ranges from 1×10^4 to1.5×10^5.

Since the average Doppler error is 1×10^{-5} m/s as shown in Fig.6, the average velocity error is from 1×10^{-4} m/s to 1.1×10^{-3} m/s in 2D-velocity, and from 0.1 m/s to 1.5 m/s in 3D-velocity. Therefore, the least squares iteration process for 3D-velocity of indoor array pseudolites can't converge.

B. Z-AXIS DEVIATION OF KNOWN POINT

The statistical method based on known points is used to analyze the positioning error because of Z-axis deviation of KPI. The analytic procedure is shown in Fig.11(a), a deviation from -1.5 m to 0.9 m is added to the Z-axis of the initialized known points. Fig.11(b) shows the positioning result from the starting point 68 to the endpoint 69. It can be seen from the positioning error of TABLE 3 that the maximum positioning error is 0.311 m in X axis, 0.08 m in Y axis. Therefore, the Z-axis of the initialized known points can be assigned an approximate value for pedestrian indoor positioning. Compared with the traditional ambiguity resolution method, the Z-fixed algorithm can reduce the user's operation complexity and enhance the continuity of positioning results.

TABLE 3. Positioning error at endpoint 69.

Z of KPI (m)	Error of X-axis (m)	Error of Y-axis (m)
2.4	-0.166	0.007
2.1	-0.116	0.005
1.8	**-0.063**	**0.003**
1.5	**-0.007**	**0.001**
1.2	**0.052**	**-0.001**
0.9	0.113	-0.003
0.6	0.178	-0.005
0.3	0.243	-0.006
0.0	0.311	-0.008

C. HORIZONTAL DEVIATION OF KNOWN POINT

A deviation from -5 m to 5 m is added to the X-axis and Y- axis of the initialized known points as shown in TABLE 4 and Fig.12, which cause a horizontal and non-linear offset of the positioning trajectory. For example, if X deviation of KPI is -5 m, and Y deviation of KPI is 0 m, then the positioning error is -2.49 m in X axis and -0.047 m in Y axis.

For pedestrian indoor positioning, an initialized known point is usually an approximate position, then the horizontal deviation tolerance of the initialized known points should be set from - 0.5 m to 0.5 m, and the maximum horizontal positioning error is less than 0.5 m.

TABLE 4. Positioning error at endpoint 69.

X deviation of KPI (m)	Y deviation of KPI (m)	Error of X-axis (m)	Error of Y-axis (m)
-5	0	-2.49	-0.047
-2	0	-1.20	-0.019
-1	0	-0.64	-0.009
1	0	0.718	0.011
2	0	1.54	0.022
5	0	4.76	0.056
0	-5	0.417	-4.38
0	-2	0.076	-1.758
0	-1	0.018	-0.878
0	1	0.002	0.877
0	2	0.044	1.747
0	5	0.345	4.300
1	1	0.725	0.926
0.5	**0.5**	**0.343**	**0.454**
0	**0**	**-0.007**	**0.001**
-0.5	**-0.5**	**-0.33**	**-0.434**
-1	-1	-0.622	-0.850

V. CONCLUSION

This paper proposes a new indoor array pseudolites positioning system. The time synchronization is not required in this system since the same clock drift of pseudolites can be estimated as an unknown parameter. Secondly, the high-precision Doppler velocity measurement and positioning method based on the Z-fixed Known Point Initialization (KPI) is developed without ambiguity resolution, and this low computational complexity method is more suitable for running on smartphone processors. Thirdly, the array indoor pseudolites can achieve centimeter level precision for dynamic and static positioning if the known points reach centimeter level precision. Finally, compared with the traditional ambiguity resolution method of indoor pseudolites, the Z-axis KPI method can be assigned an approximate value for pedestrian indoor positioning, reducing the user's operation complexity and enhance the continuity of positioning results.

In the future, the study of indoor array pseudolites will focus on the multiple access scheme [26], [27] with pseudolites network, coordinates of initial points and so on. Because the carrier phase difference measurement of indoor array pseudolites is very stable and has fingerprint characteristics which is similar to WiFi-CSI, then, some deep learning methods [28], [29] can be used to process carrier phase difference data and calculate the coordinate of initial point.

REFERENCES

[1] J. M. Stone, E. A. LeMaster, J. D. Powell, and S. Rock, "GPS pseudolite transceivers and their applications," in *Proc. Inst. Navigat. Nat. Tech. Meeting*, San Diego, CA, USA, Jan. 1999, pp. 25–27.

[2] L. K. Bonenberg, C. M. Hancock, and G. W. Roberts, "Indoor multipath effect study on the Locata system," *J. Appl. Geodesy*, vol. 4, no. 3, pp. 137–143, 2010.

[3] N. Samama, "Indoor positioning with GNSS-like local signal transmitters," in *Global Navigation Satellite Systems: Signal, Theory and Applications*, S. Jin, Ed. Rijeka, Croatia: InTech, 2012, pp. 299–338.

[4] J. Wang, "Pseudolite applications in positioning and navigation: Pro-gress and problems," *Positioning*, vol. 1, no. 3, pp. 48–56, Jun. 2002.

[5] X. Gan, B. Yu, Z. Heng, Z. Ruihui, and L. Yaning, "Pseudolite cellular network in urban and its high precision positioning technology," in *Proc. China Satell. Navigat. Conf.* Singapore: Springer, May 2017, pp. 313–324.

[6] X. Gan, B. Yu, L. Chao, and S. Liu, "The development, test and application of new technology on beidou/GPS dual-mode pseudolites," in *Proc. China Satell. Navigat. Conf. (CSNC)*. Berlin, Germany: Springer, vol. 12, 2015, pp. 353–364.

[7] N. Kohtake, S. Morimoto, and S. Kogure, "Indoor and outdoor seamless positioning using indoor messaging system and GPS," in *Proc. Int. Conf. Indoor Positioning Indoor Navigat.*, Guimarães, Portugal, Sep. 2011, pp. 21–23.

[8] D. Manandhar, S. Kawaguchi, M. Uchida, M. Ishii, and H. Torimoto, "IMES for mobile users social implementation and experiments based on existing cellular phones for seamless positioning," in *Proc. Int. Symp. GPS/GNSS*, Nov. 2008, pp. 11–14.

[9] D. Manandhar, K. Okano, M. Ishii, H. Torimoto, S. Kogure, and H. Maeda, "Development of ultimate seamless positioning system based on QZSS IMES," in *Proc. ION GNSS*, Sep. 2008, pp. 16–19.

[10] K. Fujii, Y. Sakamoto, W. Wang, H. Arie, A. Schmitz, and S. Sugano, "Hyperbolic positioning with antenna arrays and multi-channel pseudolite for indoor localization," *Sensors*, vol. 15, no. 10, pp. 25157–25175, 2015.

[11] Y. Sakamoto, H. Arie, T. Ebinuma, K. Fujii, and S. Sugano, "Hyperbolic positioning with proximate multi-channel pseudolite for indoor localization," in *Proc. IGNSS Symp.*, Jul. 2013, pp. 16–18.

[12] H. Niwa, K. Kodaka, Y. Sakamoto, M. Otake, S. Kawaguchi, K. Fujii, Y. Kanemori, and S. Sugano, "GPS-based indoor positioning system with multi-channel pseudolite," in *Proc. IEEE Int. Conf. Robot. Autom.*, Pasadena, CA, USA, May 2008, pp. 905–910.

[13] J. Wei, Y. Li, and C. Rizos, "Locata-based precise point positioning for kinematic maritime applications," *GPS Solutions*, vol. 19, no. 1, pp. 117–128, Jan. 2015.

[14] J.-E. Lee and S. Lee, "Indoor initial positioning using single clock pseudolite system," in *Proc. Int. Conf. Inf. Commun. Technol. Converg.*, Nov. 2010, pp. 575–578.

[15] J.-P. Montillet, G. W. Roberts, C. Hancock, X. Meng, O. Ogundipe, and J. Barnes, "Deploying a Locata network to enable precise positioning in urban canyons," *J. Geodesy*, vol. 83, pp. 91–103, Feb. 2009.

[16] L. K. Bonenberg, G. W. Roberts, and C. M. Hancock, "Using locata to augment GNSS in a kinematic urban environment," *Arch. Photogramm.*, vol. 22, pp. 63–74, Dec. 2011.

[17] S. Han and C. Rizos, "Improving the computational efficiency of the ambiguity function algorithm," *J. Geodesy*, vol. 70, no. 6, pp. 330–341, Jun. 1996.

[18] P. J. G. Teunissen, P. J. De Jonge, and C. C. J. M. Tiberius, "Performance of the LAMBDA method for fast GPS ambiguity resolution," *Navigation*, vol. 44, no. 3, pp. 373–383, 1997.

[19] S. Verhagen, B. Li, and P. J. G. Teunissen, "Ps-LAMBDA: Ambiguity success rate evaluation software for interferometric applications," *Comput. Geosci.*, vol. 54, pp. 361–376, Apr. 2013.

[20] J.-P. Montillet, L. K. Bonenberg, C. M. Hancock, and G. W. Roberts, "On the improvements of the single point positioning accuracy with Locata technology," *GPS solutions*, vol. 18, pp. 273–282, Apr. 2014.

[21] Y. Zhao, P. Zhang, J. Guo, X. Li, J. Wang, F. Yang, and X. Wang, "A new method of high-precision positioning for an indoor pseudolite without using the known point initialization," *Sensors*, vol. 18, no. 6, pp. 1977–1996, Jun. 2018.

[22] X. Li, P. Zhang, J. Gguo, J. Wang, and W. Qiu, "A new method for single-epoch ambiguity resolution with indoor pseudolite positioning," *Sensors*, vol. 17, no. 4, pp. 921–938, Apr. 2017.

[23] K. Fujii, R. Yonezawa, Y. Sakamoto, A. Schmitz, and S. Sugano, "A combined approach of Doppler and carrier-based hyperbolic positioning with a multi-channel GPS-pseudolite for indoor localization of robots," in *Proc. Int. Conf. Indoor Positioning Indoor Navigat.*, Oct. 2016, pp. 1–7.

[24] D. Yun and C. Kee, "Centimeter accuracy stand-alone indoor navigation system by synchronized pseudolite constellation," in *Proc. 15th Int. Tech. Meeting Satell. Division Inst. Navigat.*, Portland, OR, USA, Sep. 2002, pp. 213–225.

[25] J. D. Bard and F. M. Ham, "Time difference of arrival dilution of precision and applications," *IEEE Trans. Signal Process.*, vol. 47, no. 2, pp. 521–523, Feb. 1999.

[26] G. Gui, H. Sari, and E. Biglieri, "A new definition of fairness for non-orthogonal multiple access," *IEEE Commun. Lett.*, vol. 23, no. 7, pp. 1267–1271, May 2019.

[27] G. Gui, H. Huang, Y. Song, and H. Sari, "Deep learning for an effective nonorthogonal multiple access scheme," *IEEE Trans. Veh. Technol.*, vol. 67, no. 9, pp. 8440–8450, Sep. 2018.

[28] Y. Wang, M. Liu, J. Yang, and G. Gui, "Data-driven deep learning for automatic modulation recognition in cognitive radios," *IEEE Trans. Veh. Technol.*, vol. 68, no. 4, pp. 4074–4077, Apr. 2019.
[29] J. Wang, Y. Ding, S. Bian, Y. Peng, M. Liu, and G. Gui, "UL-CSI data driven deep learning for predicting DL-CSI in cellular FDD systems," *IEEE Access*, vol. 7, pp. 96105–96112, 2019.

XINGLI GAN was born in Tangshan, Hebei, China, in 1981. He received the B.S. degree in water supply and sewerage engineering and the Ph.D. degree in navigation, guidance, and control engineering from Harbin Engineering University, in 2004 and 2008, respectively.

From 2008 to 2011, he was a Research Assistant with the 54th Research Institute of China Electronic Science and Technology Group, China. Since 2009, he has been a Researcher with the State Key Laboratory of Satellite Navigation System and Equipment Technology, China. He is the author of one book, more than 40 articles, and more than 15 inventions. His current research interests include satellite navigation, pseudolites, visual positioning technology, artificial intelligence, and location service application.

Dr. Gan is a Senior Member of the China Electronics Society. He received the Prize (GLAC) and the provincial and ministerial awards in China.

BAOGUO YU was born in 1966. He received the B.S. degree in information processing from the National University of Defense Technology, China, in 1988, the M.S. degree in circuit and system from Yanshan University, China, in 1995, and the Ph.D. degree in communication and information system from the Beijing Institute of Technology, China, in 2005. He is currently a Professor and a Doctoral Supervisor, and the Chief Scientist of the 54th Research Institute of China Electronics Technology Group Corporation. He is currently the Director of the State Key Laboratory of Satellite Navigation System and Equipment Technology. His current research interests include GNSS, indoor positioning, applications of multisensor systems, and signal processing. He received many national science and technology awards. He is the Chinese Institute of Electronics (CIE) Fellow.

XIANPENG WANG was born in 1986. He received the M.S. and Ph.D. degrees from the College of Automation, Harbin Engineering University (HEU), Harbin, China, in 2012 and 2015, respectively. He was a full-time Research Fellow with the School of Electrical and Electronic Engineering, Nanyang Technological University, Singapore, from 2015 to 2016. He is currently a Professor with the College of Information and Communication Engineering, Hainan University. He is the author of over 60 articles published in related journals and international conference proceedings. His current research interests include communication systems, array signal processing, radar signal processing, and compressed sensing and its applications. He has served as a Reviewer for over 20 journals.

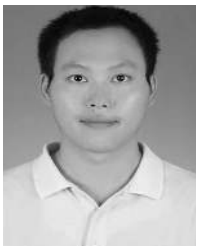

YONGQIN YANG was born in 1984. He received the Ph.D. degree from the School of Physics, Sun Yat-sen University, Guangdong, China. He is currently a Lecturer with the College of Information Science and Technology, Hainan University, Haikou, China. He is the author of over 100 articles published in related journals. His current research interests include signal processing and wireless communications, and sensor networks.

RUICAI JIA was born in 1986. He received the B.S. degree in automation from QUFU Normal University, China, in 2008, and the Ph.D. degree from Harbin Engineering University, China, in 2012. He is currently a Senior Engineer with the 54th Research Institute of China Electronics Technology Group Corporation. His current research interests include integrated navigation, and integrated navigation and pedestrian navigation. He is a CIE Fellow.

HENG ZHANG was born in Hengshui, Hebei, China, in 1988. He received the master's degree from the University of Guilin Electronic Technology, in 2016.

Since 2016, he has been a Researcher with The 54th Research Institute of the China Electronics Technology Group Corporation. He is the author of 15 articles and more than four patents. His current research interests include GNSS pseudolites, signal processing, and indoor and outdoor positioning algorithm.

CHUANZHEN SHENG was born in 1985. He received the M.S. degree in geodesy and survey engineering from the University of Chinese Academy of Sciences, Beijing, China, in 2010, and the Ph.D. degree in solid earth physics from the Institute of Geology, China Earthquake Administration, Beijing, in 2013.

From 2013 to 2015, he was an Assistant Engineer with The 54th Research Institute of the China Electronic Science and Technology Group, China. Since 2015, he has been a Senior Engineer with the State Key Laboratory of Satellite Navigation System and Equipment Technology. He is the author of more than 12 articles. His current research interests include GNSS/LEO orbit determination, GNSS time transfer, real-time kinematic positioning, precise point positioning, and GNSS deformation research.

Dr. Sheng is a Senior Member of the China Electronics Society.

LU HUANG was born in Panjin, Liaoning, China, in 1991. He received the master's degree from Harbin Engineering University, in 2017.

Since 2017, he has been a Researcher with the 54th Research Institute of China Electronics Technology Group Corporation, and with the State Key Laboratory of Satellite Navigation System and Equipment Technology. He participated in five national key research and development projects, published more than ten academic articles, and applied for three invention patents. His current research interests include multisensor fusion positioning and navigation technology, GNSS pseudolites.

BOYUAN WANG was born in 1992. He received the B.S. degree in electronics and information engineering from Harbin Engineering University, China, in 2013, where he is currently pursuing the Ph.D. degree. He is a Researcher with the 54th Research Institute of China Electronics Technology Group Corporation. His current research interests include indoor positioning, machine learning, pattern recognition, and signal processing.